IJMGE
Int. J. Min. & Geo-Eng.
Vol.48, No.1, June 2014, pp 31-54.

Application of Discriminant Analysis for Studying the Source Rock Potential of Probable Formations in the Lorestan Basin, Iran

Amir Negahdari [1], Mansour Ziaii [1], Javad Ghiasi-Freez [2*]

1. Faculty of Mining, Petroleum, and Geophysics, Shahrood University, Iran

2. Department of geology, Iranian Central Oil Fields Company (ICOFC), National Iranian Oil Company (NIOC), Iran

Received 5 January 2014; Received in revised form 14 May 2014; Accepted 16 May 2014
**Corresponding E-mail address: javadghiasi86@gmail.com*

Abstract
Understanding the performance and role of each formation in a petroleum play is crucial for the efficient and precise exploration and exploitation of trapped hydrocarbons in a sedimentary basin. The Lorestan basin is one of the most important hydrocarbon basins of Iran, and it includes various oil-prone potential source rocks and reservoir rocks. Previous geochemical studies of the basin were not accurate and there remain various uncertainties about the potential of the probable source rocks of the basin. In the present research, the geochemical characteristics of four probable source rocks of the Lorestan basin are studied using Rock-Eval pyrolysis and discriminant analysis. In achieving this goal, several discriminant functions are defined to evaluate the discriminant factor for the division of samples into two groups. The function with the highest discriminant factor was selected for the classification of probable source rocks into two groups: weak and strong. Among the studied formations, Garau and Pabdeh had the richest and poorest source rocks of the Lorestan basin, respectively. The comparison of the obtained results with the previous literature shows that the proposed model is more reliable for the recognition of the richness of source rock in the area.

Keywords: *discriminant function, Garau formation, maturity, Pabdeh formation, source rock evaluation.*

1. Introduction
British Petroleum (BP) drilled the first oil well in the Middle East in the southwest of Iran in 1908. For the first time in history, a carbonate reservoir rock had been discovered, and afterwards petroleum engineers accepted limestone as a possible reservoir rock [1]. At present, dozens of hydrocarbon fields have been discovered in Iran. The discovered fields in the south and southwest of Iran belong to the Zagros sedimentary basin. This basin is the second largest basin in the Middle East, extending along the northwest to the southwest of Iran. The Zagros sedimentary basin is one of the most important petroleum basins in the

world, mostly extending in Iranian territory and to an extent in Iraq, Turkey and Syria [2]. To date, several studies have focused on the geochemical characterization of various formations of the Zagros basin to explore probable source rocks for the accumulated petroleum within the various reservoir formations of this basin. The Sargelou, Garau-Gadvan, Kazhdomi, Gurpi and Pabdeh formations were introduced as possible source rocks of the Zagros basin. The Pabdeh formation is the main source rock only in the northeast fields of the Dezful embayment, while the Kazhdomi formation serves as a rich source rock in the southwest oilfields [3]. Gas chromatography (GC) and gas chromatography-mass spectrometry (GC-MS) have been used for the analysis of three shaly zones of the Kazhdomi formation [4]. The comparison of the obtained results and the three zones of the Asmari formation in the Marun oilfield have shown that Asmari oils originated from kerogen type II deposited in Kazhdomi formation. The Zagros sedimentary basin was comprehensively studied from a geochemical standpoint and several formations were analysed in exploring their potential as a source rock [2]. All of the previous studies in the southwest of Iran have proved the possibility of shaly formations as a source rock. The Garau (Neocomian), Kazhdumi (Albian–Cenomanian), Sargelu (Middle Jurassic, Bathonian-Bajocian) and Pabdeh (Palaeocene–Eocene) formations represent shaly formations of the northern area of the Zagros basin, and are suspected as the richest and susceptible source rocks of the Lorestan basin [1]. It seems necessary to analyse different depths of these formations in detail, although there are different geochemical characteristics in different oilfields. The Lorestan basin is an important area in terms of the hydrocarbon reserves located in the northern area of the Zagros basin. There are several obscure source rocks which have been distinguished due to their complex geological structure, and limited research has been done into this area. This study tries to study the aforementioned formations of the Lorestan basin using a statistical-mathematical methodology, known as 'discriminant analysis'. To achieve this goal, the geological characteristics obtained from Rock-Eval analysis are used.

In this study, the concept of discriminant analysis is used for the development of a classification model. Discriminant analysis is a widely used multivariate statistical method. In spite of its simplicity, it performs accurately in solving engineering problems. Some of the previous research is discussed below. Richard B. Schultz employed discriminant analysis to determine which characteristics were most useful in separating mid-continental Pennsylvanian black shale types [5]. Wang et al. used pattern recognition-like discriminant analysis to predict shale lithofacies directly from conventional log data [6]. Peh et al. developed a discriminant function model and tried to set up a unique and identifiable chemical signature for the geotectonic settings of cherts from different geotectonic provinces, especially in the case where the fossil content is lacking [7]. Discriminant analysis was also used in hydrology courses as a decision method for deciphering multiple water types based on geochemical datasets [8]. In one study, discriminant analyses were used to estimate spatial variations in groundwater chemistry in eastern Croatia and to identify the main geochemical processes responsible for high arsenic (As) concentrations in the groundwater [9]. Ghiasi-Freez et al. used discriminant analysis to introduce a semi-automated classification model of pore spaces from thin section images [10].

2. Geological Setting and Stratigraphy of the Studied Area

The Zagros fold belt encompasses approximately 14 km of sediments from the Palaeozoic era to the Quaternary period. Limited information is available from the Lower Palaeozoic sedimentary period due to the absence of exposures and because most drilled wells do not reach these depths.

According to the stratigraphic column of Figure 1, it can be seen that in the Fars geological area carbonate sediments are often deposited from the Upper Palaeozoic to Tertiary sediments in most periods of the geological history [11]. On the other hand, the Lorestan geological area includes the deep part of the sedimentary basin, and often pelagic limestone and shale facies have developed in this area. The Central Zagros area, which includes the Dezful embayment, located between the deep basin of the Lorestan and Fars platforms, shows multiple regressions and progressions of the sea due to alternating carbonate and shale layers deposited in this area [12].

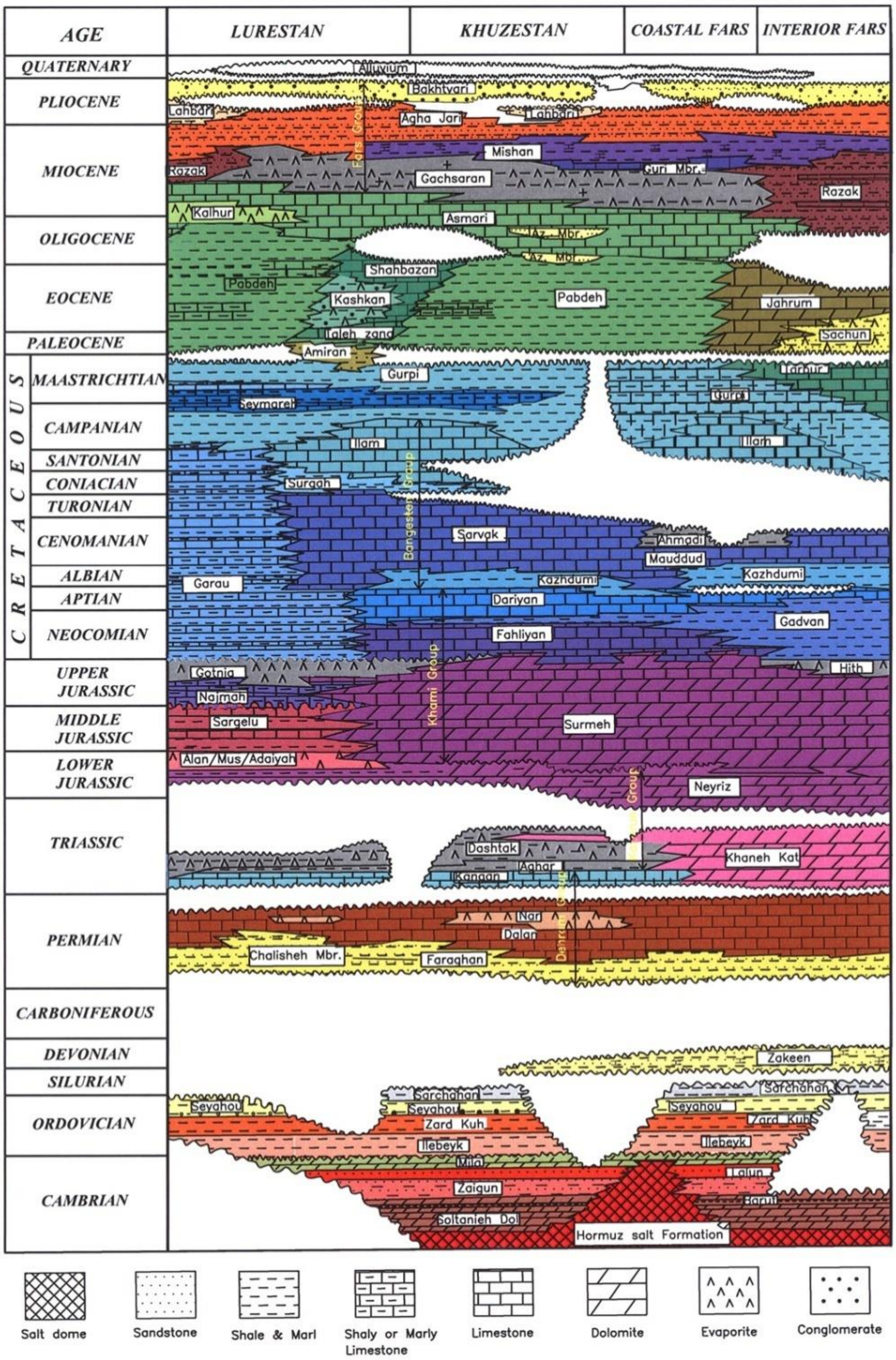

Fig. 1. Stratigraphic column of the Zagros [11].

The shaly formations of the Lorestan Basin were examined and analysed in over 10 fields. Figure 2 illustrates the location of this area on the “hydrocarbon potential areas” map of Iran. Figure 3 shows the mapping of this important hydrocarbon region. This area is located between latitude 32 to 35 north and longitude 46 to 50 east.

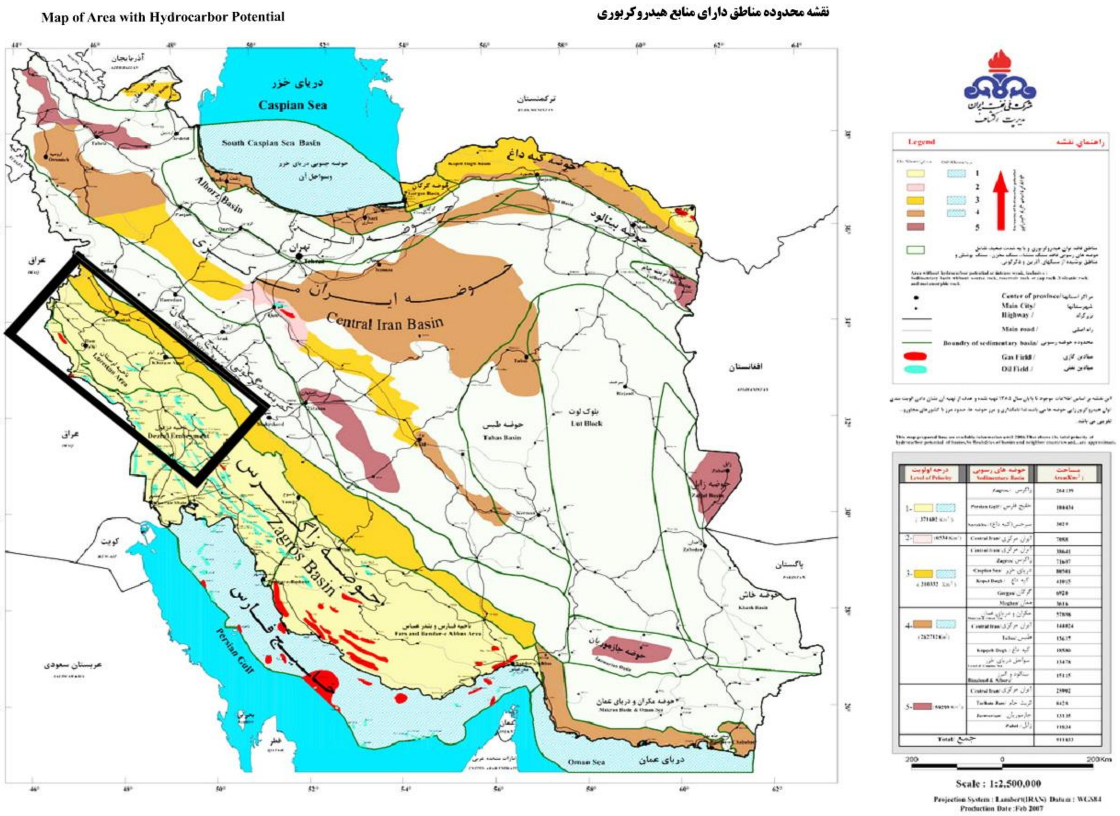

Fig. 2. Location of the Lorestan hydrocarbon basin [12].

3. Geology

The Lorestan region is part of the Zagros folded belt which is limited to the Zagros thrust fault zone from the east and northeast and from the north and northwest to the Kirkuk embayment and from the south and southeast to the Balarud bending and the Dezful embayment. The Lorestan region is part of the massive sedimentary basin of Zagros, and is extended with a length of over 1,400 km from the strait of Hormoz to Kurdistan and the borders of Iraq and Turkey. It has the greatest hydrocarbon resources in Iran and the Middle East. Figure 3 shows the structures of the Lorestan basin.

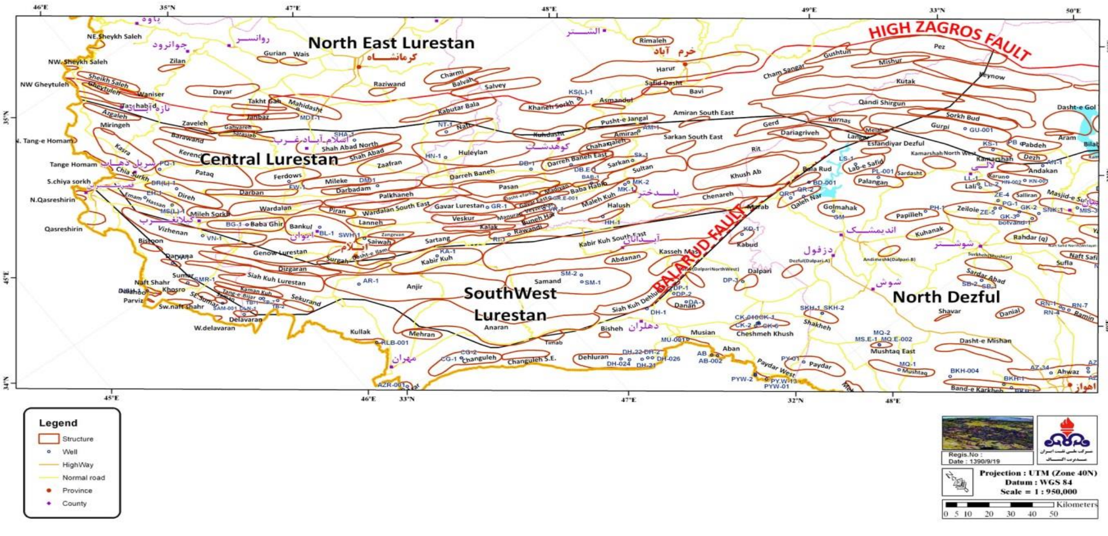

Fig. 3. The Lorestan hydrocarbon basin [12].

4. Geochemical Parameters

4.1. Rock-Eval Pyrolysis

Under the method of Rock-Eval pyrolysis, the first sample of the powdered rock is heated with an initial temperature of 300°C, and then helium - as the carrier gas - is passed through it. Next, based on a temperature schedule (at a rate of 25°C per minute), the temperature increases from 300°C to 600°C. During the pyrolysis steps, three peaks are detected by a flame ionization detector (FID), which shows the petroleum potential of the sample. The area under the first peak released at 300°C is known as S_1. Carboxylic groups of kerogen break between 300°C and 390°C and cause CO_2, which is analysed by another detector, known as TCD, and a S_3 curve is obtained. The obtained value is divided by the amount of organic carbon and this ratio is known as the 'oxygen index'. At temperatures between 300°C and 600°C, kerogen molecules available in rock will be broken and hydrocarbons produced. This hydrocarbon will be analysed by FID and peak S_2 is thus obtained. All that remains are wasted carbons or residuals. The amount of carbon residue (S_4) is calculated by the oxidation system of the device or else by using another TCD detector. The parameters are shown in Figure 4 [13].

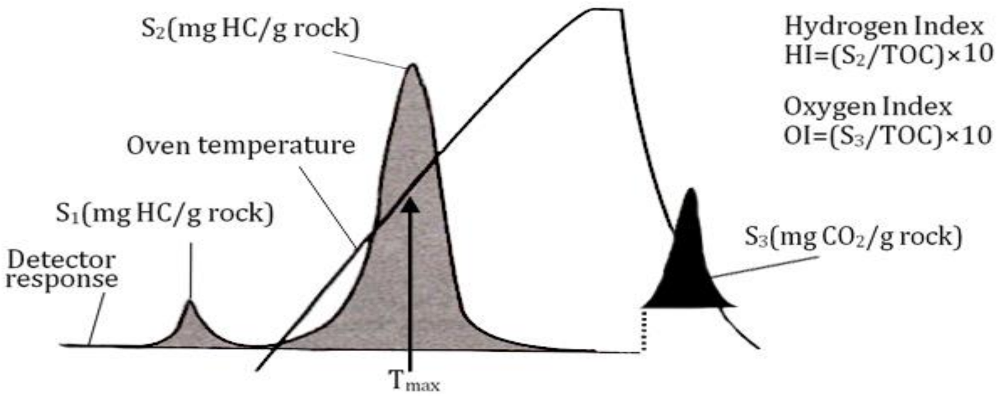

Fig. 4. Curves S_1, S_2, S_3, HI, OI and T_{max} of the source rock analysis [13].

Rock-Eval peaks show the amount of free hydrocarbons in a sample and they are calculated in milligrams of hydrocarbon per gram of rock. Free hydrocarbons may be generated due to the maturation of the kerogen of organic matter. There is another possibility which states that they might migrate from other rock layers to the understudied source rock. Before analysing the samples, they should be completely cleaned of drilling mud because they may be affected by the contamination of drilling oil base-mud.

4.2. S_2 Parameter (Hydrocarbon Producing Potential)

This parameter indicates the potential of the source rock for hydrocarbon generation. Table 1 shows the rock quality from the viewpoint of hydrocarbon generation based on the S_2 values [14]. To check the hydrocarbon-producing power remaining in the rock, an index called the 'producing potential index' can be used, which is equal to S_1+S_2.

Table 1. Rock classification based on production power and according to parameter S_2 [14].

	Poor	Fair	Good	Very good	Excellent
S_2 Values	less than 2.5	2.5-5	5-10	10-20	morethan20

4.3. Total Organic Carbon (TOC%)

This parameter indicates the richness and quantity of organic matter (Table 2). Studies reveal that the minimum required amount of organic carbon for oil and gas generation in a source rock is 1% and 0.5%, respectively [15].

Table 2. Description of the geochemical parameters of hydrocarbon producing potential [15].

Organic Matter			
Hydrocarbon Potential	TOC (weight percent)	Rock–Evil Pyrolysis	
		S_1	S_2
Poor	0 - 0.5	0 - 0.5	0 - 2.5
Fair	0.5 – 1	0.5 - 1	2.5 –5
Good	1 – 2	1 - 2	5–10
Very good	2 – 4	2 - 4	10–20
Excellent	more than 4	more than 4	more than 20

4.4. Hydrogen Index (HI)

Hydrocarbon production of kerogen reduces from type I to III. Kerogen types I and II are suitable for oil and gas production, while kerogen type III is a gas-prone kerogen (Table 3). Therefore, it is important to know the kerogen type in determining the hydrocarbon type. The HI versus the T_{max} diagram is used to determine the type of kerogen [15].

$$HI= (S_2/TOC) \quad (1)$$

Table 3. Type of kerogen based on geochemical parameters [15].

Kerogen Type / Parameter	I	II	II/III	III	IV
Hydrogen Index (mg HC/g TOC)	more than 600	300-600	200-300	50-200	less than 50
S_2/S_3(HI/OI)	more than 15	10-15	5-10	1-5	less than 1

4.5. Oxygen Index (OI)

The plot of the HI versus the OI can also be used to illustrate the type of kerogen (Fig. 5) [15]. The OI is defined as below [15]:

$$OI= (S_3/TOC) \quad (2)$$

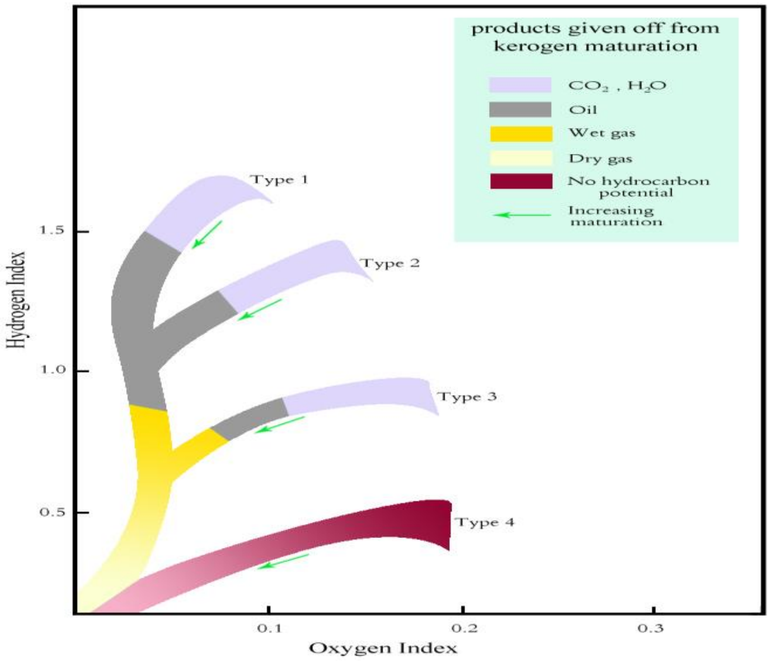

Fig. 5. Ratio of the HI to the OI [14].

4.6. The T_{max} Parameter

T_{max} is the temperature at which the maximum amount of hydrocarbon is generated during the pyrolysis process. In other words, T_{max} is the temperature at which S_2 reaches its maximum value. The T_{max} value also increases where maturity increases. Organic matter with abundant hydrogen has a low T_{max} value and a low residual, while organic matter containing low levels of hydrogen exhibits a higher T_{max} value. Figure 6 shows the graph of HI vs. T_{max} [16]. T_{max} and vitrinite reflectance (Ro) are used to indicate the level of thermal maturity of samples (Table 4).

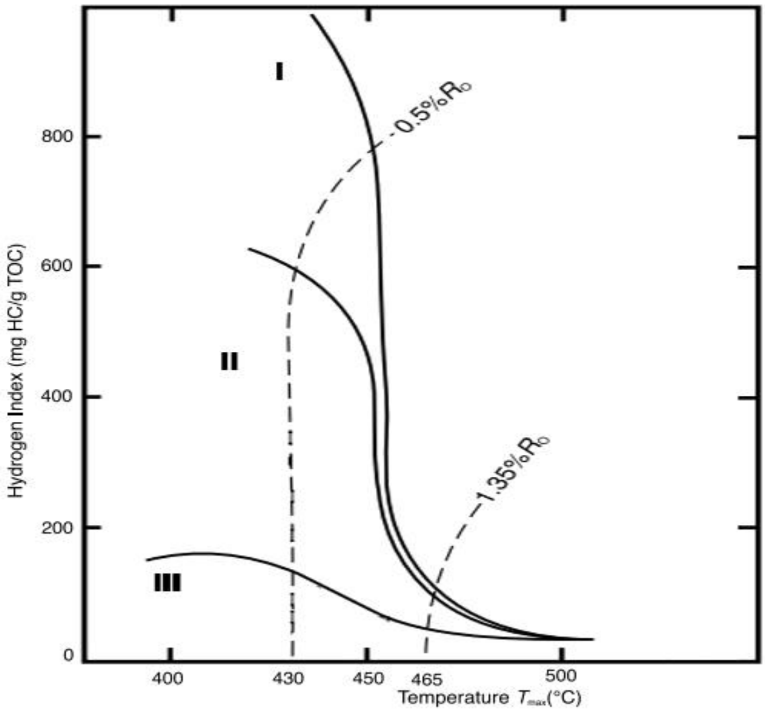

Fig. 6. Diagram of the HI to T_{max} [16].

Table 4. Geochemical parameters that indicate the level of maturity [15].

		Maturity Parameters	
Level of Thermal Maturity		% Ro	T_{max} (^{o} C)
Immature		0.2-0.6	less than 435
Mature	Early Mature	0.6-0.65	435-445
	Peak of Mature	0.65-0.9	445-450
	Late Mature	0.9-1.35	450-470
	Post Mature	more than 1.35	more than 470

4.7. Production Index

The production index is predicated as the ratio of hydrocarbon present in the rock (S_1) to the total hydrocarbons measured in the pyrolysis stage (S_1 + S_2) [13].

$$PI = S_1/ (S_1 + S_2) \tag{3}$$

The power factor of (genetic) hydrocarbon production is defined as [13].

$$PP= (S1+S2) \tag{4}$$

The production index appears from 1.0 at the beginning of the oil generation stage (shallow depths) reaching 4.0 at the end of the oil generation stage (greater depths). Thus, the production index can be used as a maturity parameter. If S_2 is very low, PI will be (abnormally) very high.

In this section, the NIOC source rock data and elements of Kavoosi et al.'s 2011 [12] studies are used. Next, based on these, the probable shaly formations of the Lorestan basin are analysed.

5. Geochemical Characteristics of the Studied Formations

5.1. Pabdeh

A) Total Organic Carbon (TOC%)

The TOC percentage of the Pabdeh samples, taken from the drilled wells, shows a wide range of TOC (from 0.11% up to 6%). The maximum values of the TOC among the analysed samples are in the samples from the Maroon oilfield's wells, ranging between 20.36% and 6.59%, and the minimum values are measured in the Babaghir and Asmari wells, ranging from 0.11% to 1.16%. In general, in most of the wells, the collected TOC values of the samples in the Pabdeh formation are very good.

B) Hydrogen Index (HI)

This value is related to the maturity of samples. The maturity of a sample is due to a high temperature, which results in the production of hydrocarbons; hence, the HI values of the samples will be reduced. Accordingly, in order to interpret the HI values of the samples, we should consider their T_{max} as well.

The HI values of the samples from the Pabdeh formation are highly variant, as the maximum values are in the samples from the Ab-Tymur wells, ranging from 400 to 822 (mg HC/ g TOC), while the minimum values are in the Asmari wells and some of the Babaghir wells, which are less than 100 (mg HC/ g TOC).

Generally, the Pabdeh formation has variant HI values as it contains many different facies. In addition, hydrocarbon production in this formation is qualitatively good. We can say that the Pabdeh formation could serve as a good source rock.

C) Maturity and Organic Matter (T_{max})

T_{max} can be considered as the temperature at which all of the organic matter (kerogen) in the source rock transforms into hydrocarbons.

The results from Rock-Eval show that the maturity of the Pabdeh samples is mostly in the immature stage - in other words, their T_{max} values are less than 435 ^{o}C. The maximum maturity among the samples of the Pabdeh formation is associated with samples taken from the Asmari wells, where T_{max} is greater than 450. In spite of this, the Pabdeh formation in the Babaghir, Palangan and Kabud wells is at the hydrocarbon production stage (oil zone), while the Ziluie, Ghale-Nar, Haft-kel and Kupal wells are at the early stages of the oil window. Note that very small amounts of HI and TOC in the Pabdeh formation samples and in the Asmari well result in incorrect T_{max} values [12].

Generally, the Pabdeh formation - except for aforementioned wells - sees most of its wells at the immature stage or else at the beginning of the oil window (Fig. 7).

D) Kerogen Type

In order to identify the type of kerogen, in the analysed samples from Pabdeh, we use van Krevelen, maturity parameters (T_{max}) and the HI from Rock-Eval. All the Pabdeh samples from different wells are plotted on the standard diagram of T_{max} VS HI, which is shown in Figure 7. This Figure shows that the kerogen presented in the Pabdeh samples is of marine type (type II) with some continental organic materials (type III). Another result is that the hydrocarbon potential of the Pabdeh samples is so different that the HI values fluctuate between 50 and 600. These show the dramatic variation in the facies or lithology in the Pabdeh formation and represent the diverse potential of the samples. The T_{max} values shown in this diagram indicate that most of the samples are at the immature stage. Despite this, some of the samples in wells such as Ghale-Nar, Ziluie and Kabud are in hydrocarbon production. The minimum maturity of the Pabdeh formation is found in the samples from the Janguleh well, where the T_{max} value ranges from 400 to 410.

E) Hydrocarbon Potential

In order to identify the hydrocarbon production potential of source rocks, graphs are used showing PP = (S_1 + S_2) Vs. TOC. Accordingly, the greater the TOC and PP in the source rocks, the greater the hydrocarbon production potential of the source rock. This concept is used in identifying the hydrocarbon potential of the Pabdeh formation in the wells in the Lorestan and Dezful areas. The TOC and PP ratio of all the samples of the Pabdeh formation taken from the Dezful wells in addition to the Babaghir well in Lorestan are depicted in the aforementioned diagram, shown in Figure 8. According to the results, it can be seen that the Pabdeh formation in northern Dezful has a very high hydrocarbon potential, while the formation in Lorestan (the Babaghir well) performed weakly.

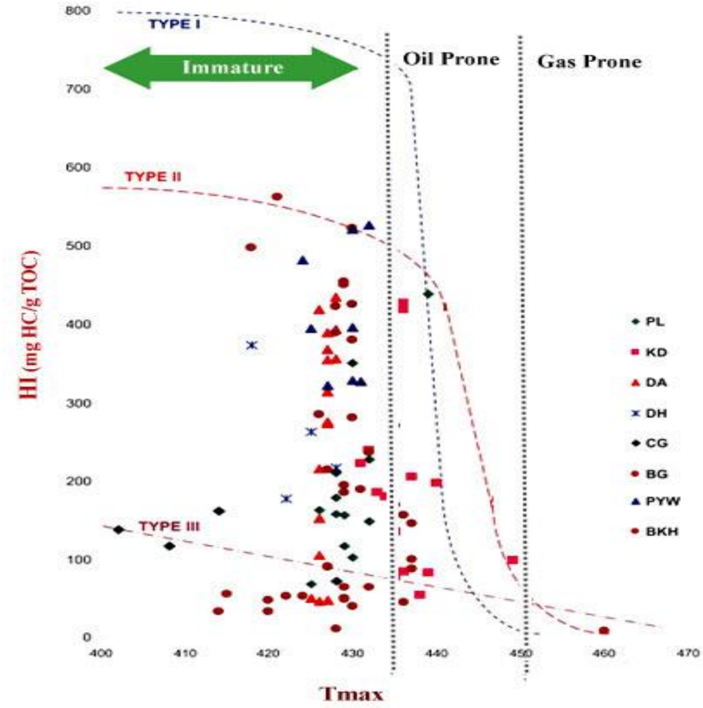

Fig. 7. Graph of HI VS T_{max} in the Pabdeh samples [12].

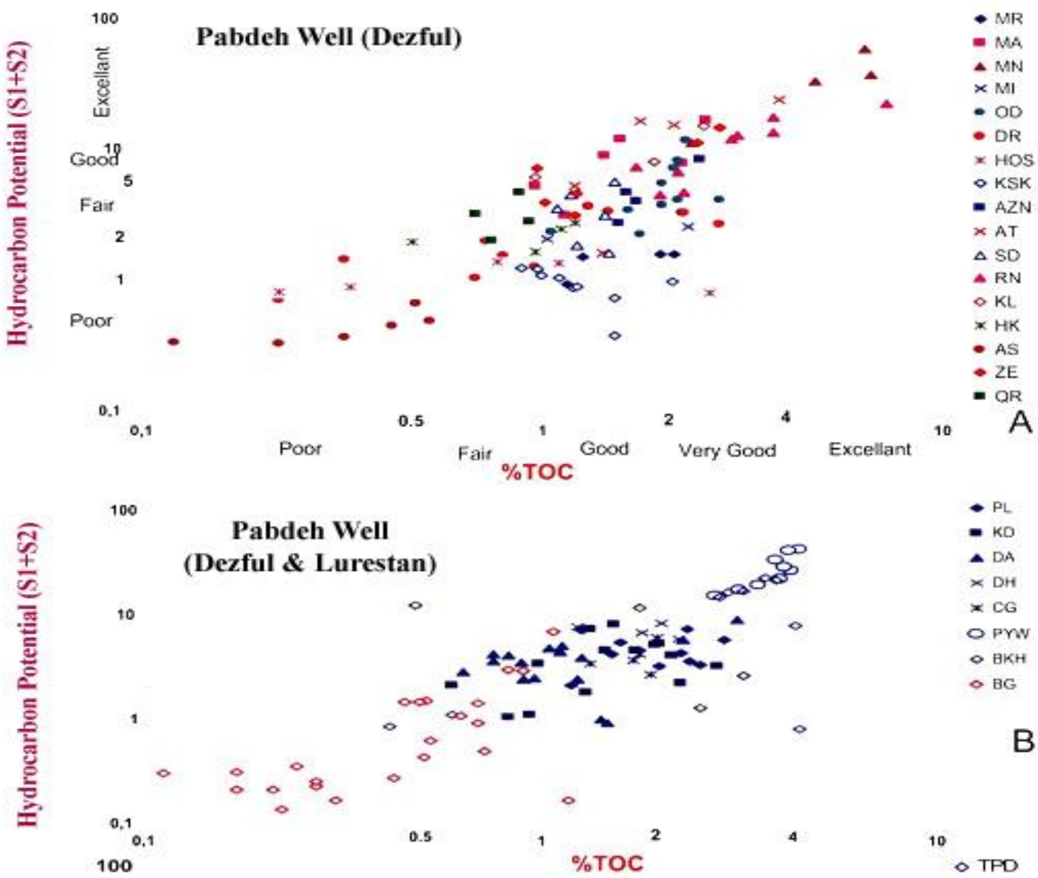

Fig. 8. Diagram of the PP and TOC ratio of the Pabdeh formation samples [12]

5.2. Kazhdumi

According to the results of Rock-Eval, 93 samples of the Kazhdumi formation obtained from 15 wells were studied.

A) Total Organic Carbon (TOC %)

The TOC obtained from the Kazhdumi formation samples varied from 1% to 5%. The maximum TOC was found in the samples of the Susangerd, Ahwaz, Maroon and Mansouri wells, varying from 4% to 8%, while the minimum one which was obtained from the samples of the Omid, Azadegan and Dehloran wells varied from 0.5% to 1.5%. The TOC of the Kazhdumi samples in most wells was very good and without any change in organic matter, showing the homogeneity of the facies and the sedimentation environment in this formation.

B) Hydrogen Index (HI)

The HI of the Kazhdumi formation samples varied among the wells, seeing a maximum value of 400 to 800 in the Hosseinie and Susangerd wells and a minimum value of 100 mg HC/g TOC in the samples of the Danan and Kushk wells. The reason for such considerable variation in value of the HI in the Kazhdumi samples might be the maturity of the samples due to a decrease of this value and the absence of organic matter in the formation facies. First, the value of the HI should be compared with the T_{max} of the samples to control for it.

C) Maturity of Organic Matter (T_{max})

Based on analyses of Rock-Eval, most of the analysed samples which were taken from Kazhdumi Formation in various wells are in various maturity stages of hydrocarbon production that is their T_{max} is above 435. The maximum maturity value of Kazhdumi Formation samples is related to Haft-kel, Maroon, Mamatin, Mansouri and Changuleh wells indicating a T_{max} of 440. The minimum maturity degree of Kazhdumi Formation samples relates to samples of Hosseinie, Kushk and Azadegan wells which are approximately 435.

D) Kerogen Type

Van Krevelen standard curves are used to identify the type of kerogen which forms the organic matter in the analysed samples of the Kazhdumi formation. The maturity parameters (T_{max}) and HI, which were obtained from Rock-Eval analyses, can be found on the axes of Figure 9.

All of the samples of the Kazhdumi formation from different wells are drawn on the standard diagram of T_{max} vs. HI. As the Figure shows, the kerogen of the organic matter in the Kazhdumi formation is marine (or kerogen type II) along with terrestrial kerogen (type III). The values of the HI which identify the hydrocarbon potential of the Kazhdumi formation are also very diverse. In addition, based on the value of T_{max} and the maturity of the samples, most of the samples were at the stage of producing hydrocarbon and/or at the stage of oil production.

E) Hydrocarbon Potential

Samples of the Kazhdumi formation in the wells of northern Dezful indicate the good-to-excellent potential of the hydrocarbons.

In this study, the samples of the Kazhdumi formation relating to the Maroon, Ahwaz, Mahshahr, Mansouri, Omid and Hosseinieh wells indicate the excellent potential of hydrocarbons, while the samples of the Kushk, Dehloran and Danan wells have the lowest potential.

In general, the hydrocarbon potential of the Kazhdumi formation in northern Dezful varies from very good to excellent, based on the values of the TOC and the PP (Fig. 10).

5.3. Garau

122 samples taken from the Garau formation were analysed by Rock-Eval.

A) Total Organic Carbon (TOC %)

The TOC of the samples of the Garau formation taken from wells in Lorestan is highly variant, ranging from weak (below 0.5%) to excellent (5%). The minimum percentage TOC is found in some of the samples from the Anjir, Babaghir, and Mahidasht wells. It is necessary to note that the TOC percentages in the samples of a well are varied. This means that the facies of the Garau formation did not obtain in an equally homogenous sedimentary environment and same lithoilogy.

The samples of the Garau formation in northern Dezful, including the Darkhuin, Kushk, Haftkel and Dehloran wells, have a higher mean TOC than the Garau samples in Lorestan. The TOC percentages for the Garau Formation in the northern Dezful wells vary from 1% to 6.4 % while this rate is below 1% for the samples of the Dehloran well.

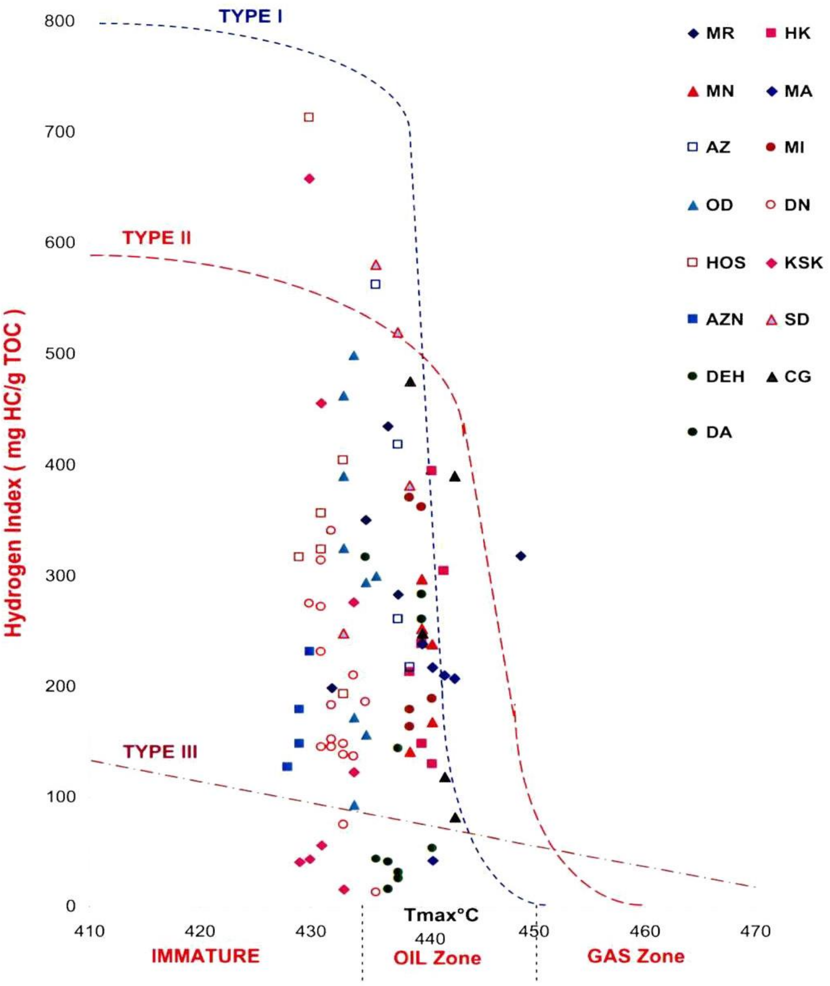

Fig. 9. Graph of HI VS T_{max} in the Kazhdumi samples [12].

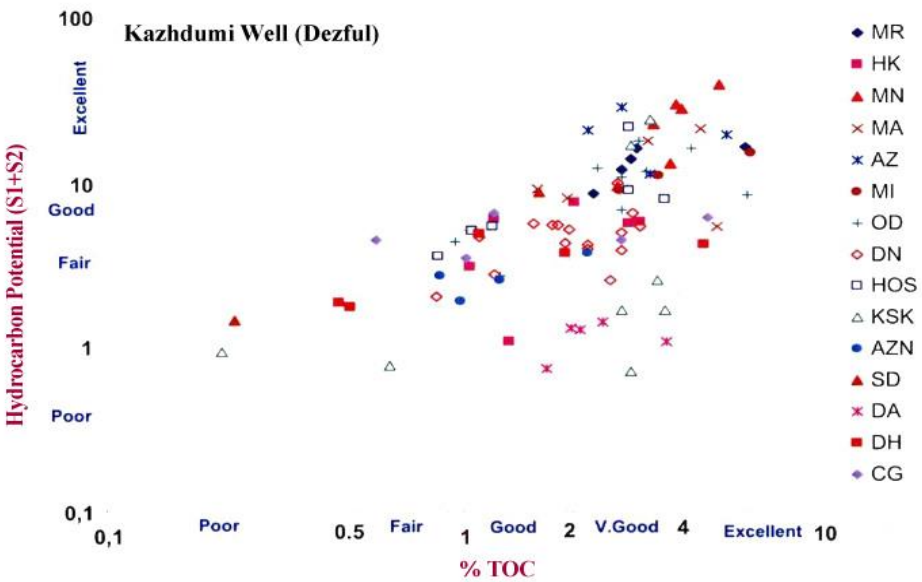

Fig. 10. Diagram of the PP and TOC ratio of the Kazhdumi formation samples [12].

B) Hydrogen Index (HI)

To assess the HI of the source rock samples, their T_{max} should be considered. The results obtained from samples of the Garau formation in the northern Dezful wells indicate that this formation has a relatively good HI rate in this region, with considerable variations among the samples (approximately 45-445 mgHC/grock). The mean HI value of the Garau formation samples in the wells of the Lorestan region is below the related value of the samples taken from the northern Dezful wells, and their calculated value varies from 10 to 200 mgHC/grock, and only a few samples of the Garau formation in the Vinahar and Babaghir wells have a higher HI.

C) Maturity of Organic Matter (T_{max})

T_{max} results of the analysed samples of the Garau formation in northern Dezful strongly indicate that most of the samples taken from the Darkhoein, Kushk, Haftkel and Dehloran wells have a high maturity rate while their T_{max} is found in the oil production zone (oil zone) Results obtained from the samples of the T_{max} of the Garau formation in the Lorestan wells almost indicate a very high maturity rate, for which the T_{max} value is above 440°C and less than 460°C. Most of the samples of the Garau formation in Lorestan are found in the oil zone and/or at the beginning of the gas production zone. Therefore, it is necessary to note that the HI rates of most samples range from 'very weak' to 'weak' (0 to 100), indicating that a proportion of the hydrogen available in the samples had changed to hydrocarbon due to the high maturity level and considerably reduced HI (or else were due to the conditions of the original sedimentary environment and protected organic matter which kept the HI level low). Therefore, it exhibits a high T_{max}.

D) Kerogen Type

To identify the type of kerogen in the organic matter comprising the Garau formation, standard geochemical graphs are used consisting of T_{max} and the HI. All the samples of the Garau formation obtained from different wells (in the Lorestan region) are drawn on the van Krevelen diagram, as shown in Figure 11.

As shown in the Figure, most of the samples have an approximate T_{max} of 435°C to 450°C as well as diverse HI values, varying from 0 to 600. This indicates that the samples are found in the final stage of the oil zone and that they have various hydrocarbon production potentials. According to the diagram in Figure 11, the kerogen type of the Garau formation is marine (type II) along with a small amount of terrestrial organic matter.

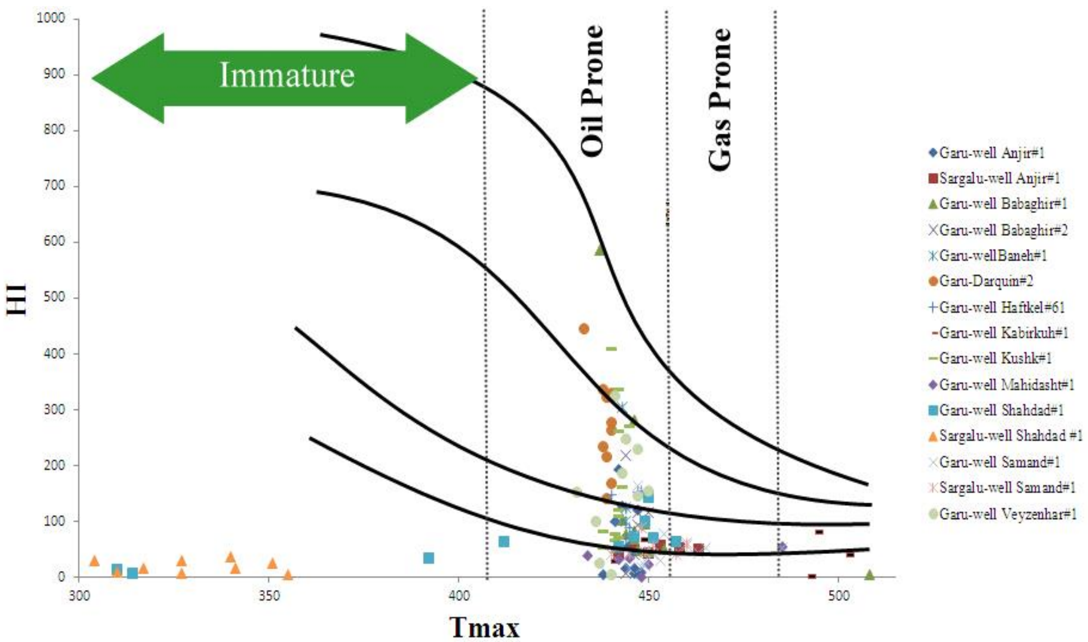

Fig. 11. Graph of the HI VS T_{max} for samples of the Garau and Sargelu formations in the Lorestan region.

E) Hydrocarbon Potential

To identify the primary hydrocarbon potential of the source rock, a geochemical diagram is used based on the geochemical indices PP = (s1+s2) and TOC.

Most of the samples of the Garau formation in the Lorestan wells have weak hydrocarbon potential (PP<2) but have TOC rates varying from weak to very good. Some of the samples which have been obtained from Darreh Baneh, Viznharand and northern Shah Abad, have medium hydrocarbon potential. As shown in Figure 12, Part B, the results obtained from the samples of the Garau well in northern Dezful exhibit medium-to-good hydrocarbon potential (2 to 10 PP) and a medium-to-excellent TOC percentage.

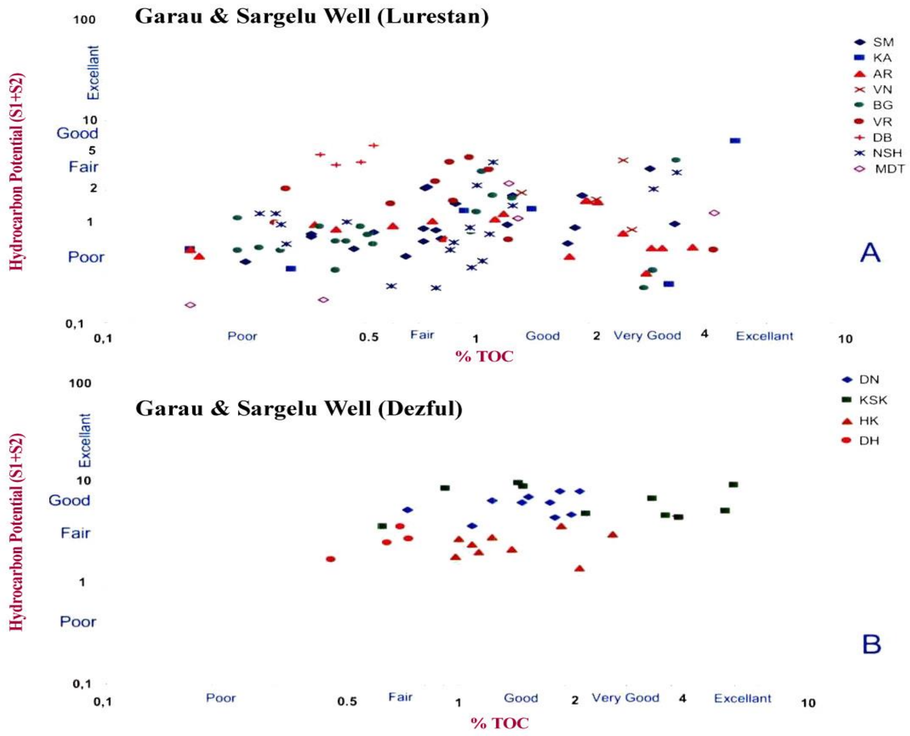

Fig. 12. Diagram of the PP and TOC ratio of the Garau and Sargelu formation samples [12].

5.4. Sargelu

Only 24 samples of the Sargelu formation, obtained from five wells, are analysed by the Rock-Eval method.

A) Total Organic Carbon (TOC%)

There are various rates of TOC in the samples of the Sargelu formation taken from the Lorestan region's wells, including the Samand, Anjir, Shah Abad, MahiDasht and Mulilan wells, ranging from weak (less than 0.5%) to excellent (more than 5%).

It is necessary to note that there are diverse variations in the TOC percentage in the samples of Sargelu in one well, indicating that Sargelu does not have unique facies or lithology. TOC value of two samples is the same in Darkhuin well. (1.94 and 1.58).

B) Hydrogen Index (HI)

The T_{max} values should be considered in evaluating the rate of the HI of the samples taken from the source rock. The HI of the samples taken from the Sargelu wells of the Lorestan region is relatively weak and varies between 0 and 60 (mgHC/grock).

C) Maturity of Organic Matter (T_{max})

The T_{max} results of the analysed samples taken from the Sargelu formation indicate a high maturity level in all of the wells of the Lorestan region, while their value is high in the oil zone (and even at the beginning of the gas zone) at between 440 °C and 460 °C. Samples of the Sargelu well in northern Shah Abad also have a T_{max} between 330 °C and 350 °C at the immature level, which is unusual considering their depths. Two samples of the Sargelu wells which have been obtained from Darkhuin well are found in the oil zone and have a T_{max} ranging from 439 °C to 440 °C.

6. Statistical Analysis of the Geochemical Parameters

6.1. The Pabdeh Formation

There are 25 wells drilled in the region drilled to this formation and 195 samples were obtained and analysed with the Rock-Eval machine. Sixty samples (30.77% of these samples) had over 2% TOC and their mean was 3.09%. The total mean organic carbon in all the samples was 1.68% (Fig. 13a).

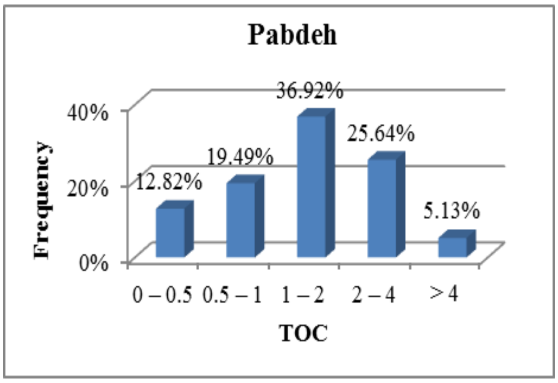

Fig. 13a. TOC Frequency of Pabdeh Formation.

Twenty-three of the 195 samples were at the early maturity stage based on their T_{max} and eight of them had a higher maturity level. This includes 15.9% of all the samples (Fig. 13b).

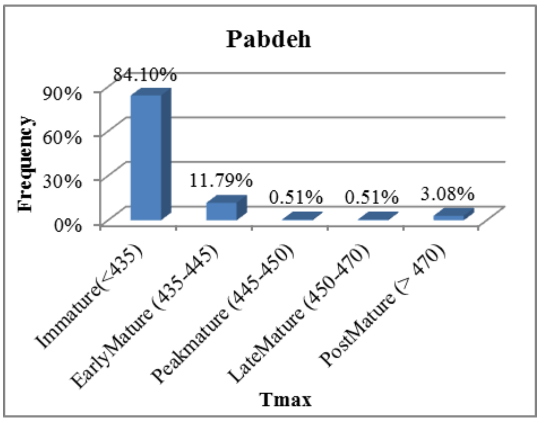

Fig. 13b. Maturity of the Pebdeh samples according to $T_{max.}$

The mean value of the vitrinite reflectance of all wells is 43% (Fig. 13c).

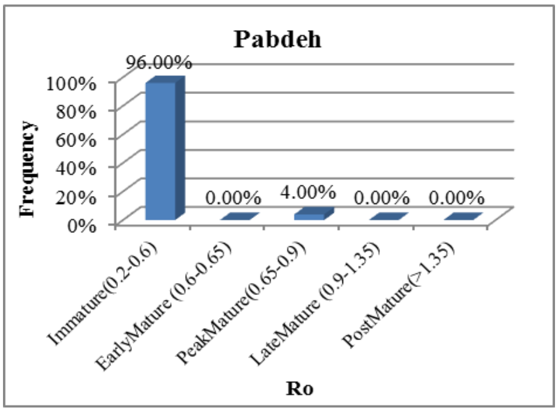

Fig. 13c. Maturity of the Pabdeh samples according to Ro.

Based on the HI values, the predominant kerogen in this formation is of type III and then type II, or else a combination of the two types, indicating a high potential for the production of gas (Fig.13d).

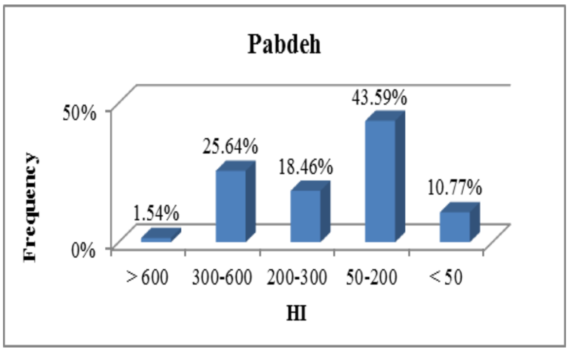

Fig. 13d. Frequency of the HI in Pabdeh.

6.2. The Kazhdumi Formation

The Kazhdumi formation has been drilled for 15 wells in Lorestan and northern Dezful, and in total 93 samples were obtained from this formation. The mean TOC of this formation was 2.65% and 58 samples had a TOC above 2% (Fig. 14a).

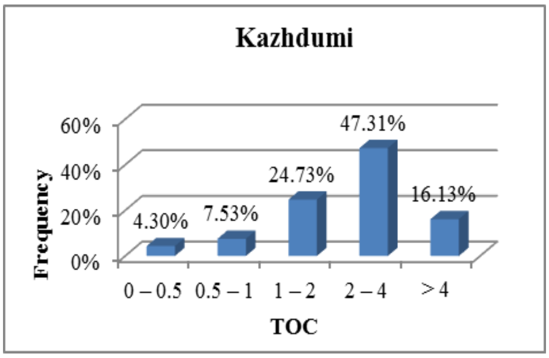

Fig. 14a. TOC frequency of the Kazhdumi formation.

The T_{max} of this formation is 435.98˚C and 53 of these 93 samples had a temperature higher than 435°C and a mean of 439.17. This represents the low maturity of the formation (Fig. 14b).

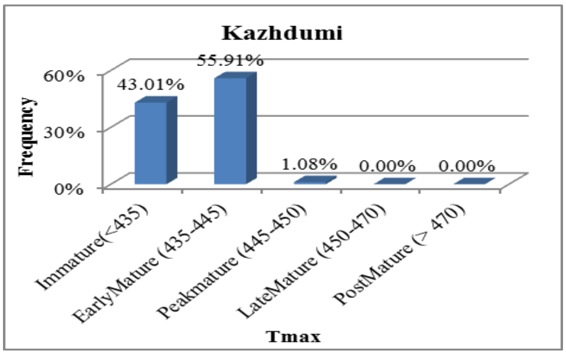

Fig. 14b. Maturity of the Kazhdumi samples according to T_{max}.

The mean value of the vitrinite reflectance of the Kazhdumi formation in these 15 wells was 65% and the mean value of the samples was between 51.8% and 88.2% (Fig. 14c).

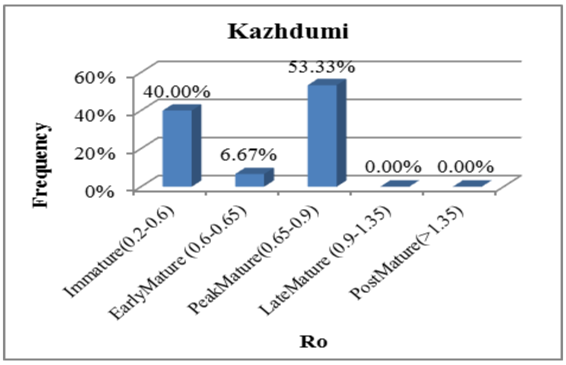

Fig. 14c. Maturity of the Kazhdumi samples according to Ro.

Considering the HI values, 87% of the samples in this formation varied from 50 to 600 mg of the organic matter (Fig. 14d).

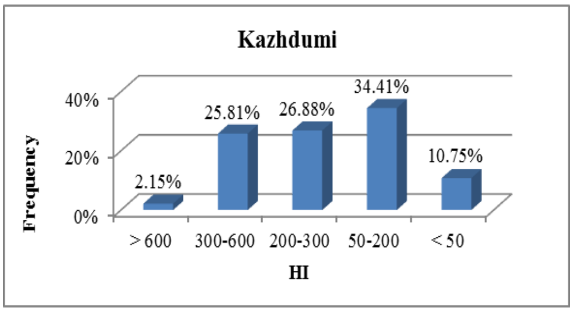

Fig. 14d. Frequency of the HI in Pabdeh .

6.3. The Garau Formation

Fifteen wells have been drilled in the Garau formation and their data are available. One-hundred and twenty-two samples of these wells were obtained and analysed using Rock-Eval.

The TOC of these 122 samples ranged between 0.17 % and 10.8%, and the mean value was 1.78%. Thirty-three of these 122 samples had a TOC of more than 2% and the TOC mean value was 3.88% (Fig. 15a).

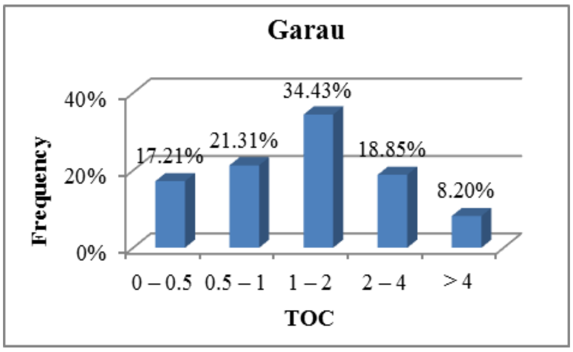

Fig. 15a. TOC frequency of the Garau formation.

The Garau formation also has a high maturity level because 114 samples (i.e., 93%) have a T_{max} greater than 435 °C and a mean value of 447.44 °C (Fig. 15b).

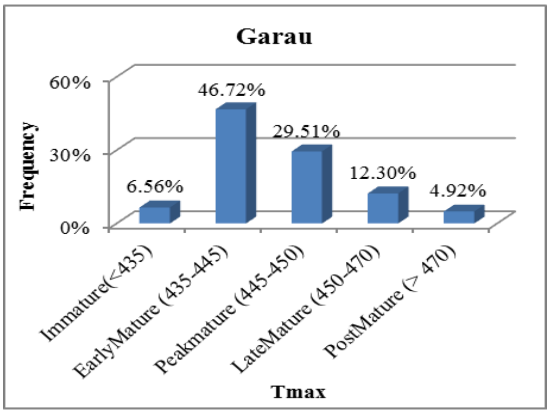

Fig. 15b. Maturity of the Garau samples according to T_{max}.

The mean value of the vitrinite reflectance was also found in 15 samples, among which five samples had a mean higher than 1.0% while the mean value of all of them is 94% (Fig. 15c).

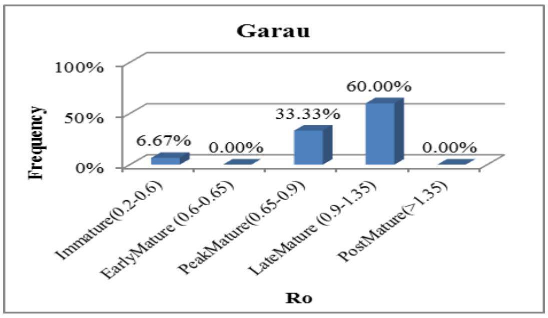

Fig. 15c. Maturity of Pabdeh samples according to Ro.

Considering the HI value of the Garau formation, it is assumed that the predominant kerogen is of types III and IV because around 82% of the samples have a TOC lower than 200 mg. However, it is necessary to note that the reduction of the HI is due to the production of hydrocarbon, considering high TOC and high maturity level, because hydrogen decreases when hydrocarbon is produced (Fig. 15d).

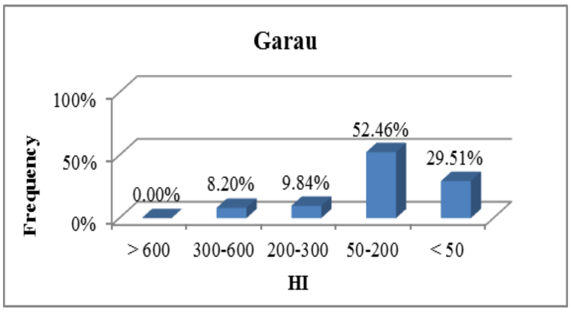

Fig. 15d. Frequency of the HI in Garau.

6.4. The Sargelu Formation

Only a few samples were taken from this formation for study. The Sargelu formation was drilled in five wells and 24 samples were obtained with the following results obtained from the Rock-Eval analysis:

The mean value of the TOC of the samples was 1.35% and seven samples had a TOC greater than 2% and a mean of 2.49 (Fig. 16a).

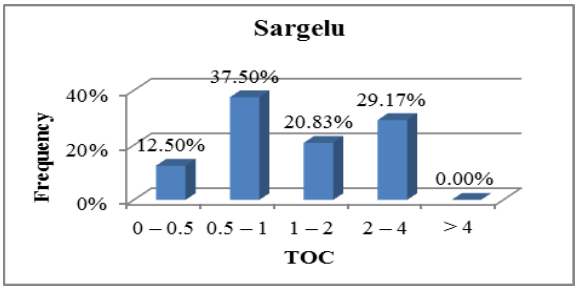

Fig. 16a - TOC frequency of the Sargelu Formation.

The mean value of T_{max} was 411.87 and 16 samples had a T_{max} higher than 435 °C and a mean of 451 °C. The maturity level of this formation is relatively high. On the other hand, the mean values of the vitrinite reflectance were obtained in five wells and the mean value was 1.42% (Fig. 16b and 16c).

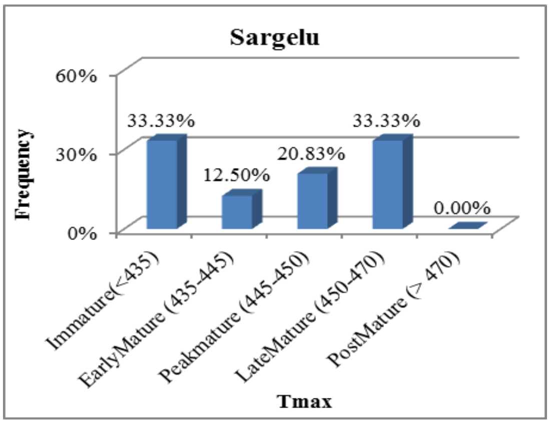

Fig. 16b. Maturity of the Sargelu samples according to T_{max}.

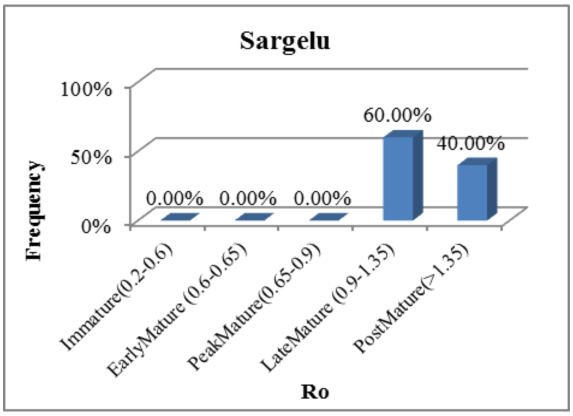

Fig. 16c. Maturity of the Sargelu samples according to Ro.

This formation is almost equal to the Garau formation. This means that the measured values are below 200 (Fig. 16d).

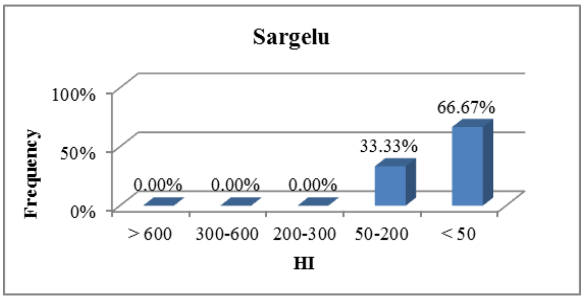

Fig. 16d. Frequency of the HI in Sargelu.

7. Methodology

7.1. Discriminant Analysis

Discriminant analysis is a statistical method for the classification of data and the combination of a variety of information regarding an issue. Interesting applications can be found in almost every traditional scientific area, ranging from the social sciences to the health sciences, and from industry to the economy. The method is a supervised process based on training data which corresponds to a vector of input data with a particular class of output, and it trains a function as a discriminant function. Each of these functions is composed of a set of weights and coefficients based on which the numerical value of each of the functions is calculated using the numerical value of features extracted and then based on Bayes theory; the function that is most likely to be accounted for indicates the class corresponding to the input vector. The mathematical basis of this method is as follows.

Assuming that the discriminant function and its corresponding probability value can be displayed with H and P, respectively [19],

$$H_i(x) = p(C_i \mid X) \tag{5}$$

According to Hastie et al. [19], this relationship can be extended as follows.

$$H_i(X) = \ln p(X \mid C_i) + \ln p(C_i) \tag{6}$$

In the above expression, the value of P (X|Ci) is expanded as follows [19].

$$p(X \mid C_i) = \frac{exp^{-(x-\mu_i)^T \times (x-\mu_i)/2\sum_i}}{\sqrt{(2\pi)^n \times \left|\sum_i\right|}} \tag{7}$$

Therefore, the general form for a discriminant function will be as follows [19].

$$H_i(X) = -\frac{(x-\mu_i)^T \times (x-\mu_i)}{2\sum_i} - \frac{n}{2} \times \ln(2\pi) - \frac{\ln\left|\sum_i\right|}{2} + \ln p(C_i) \tag{8}$$

The linear form is the simplest form of eq. (8) that can be used when the extraction features follow a certain order. The linear form of the equation is [19].

$$H_i(X) = -\frac{X^T \times \mu_i}{\sum} - \frac{\mu_i^T \times \mu_i}{2\sum} + \ln p(C_i) \tag{9}$$

In the case of data irregularity, the performance of the analysis will be better for other forms of the equation, such as quadratic form. The quadratic form of the discriminant analysis equation is [19].

$$H_i(X) = -\frac{(x-\mu_i)^T \times (x-\mu_i)}{2\sum_i} - \frac{\ln\left|\sum_i\right|}{2} + \ln p(C_i) \tag{10}$$

In the above equations, the numerical values of P(Ci), μ and Σ are calculated using the following relations [19].

$$p(C_i) = {n_i}/{N} \tag{11}$$

$$\mu_i = \frac{1}{n_i} \sum_{j=1}^{n_i} X_j \qquad i = 1, 2, \ldots, k \tag{12}$$

$$\sum_i = \frac{1}{n_i} \sum_{j=1}^{n_i} (X_j - \mu_i) \times (X_j - \mu_i)^T \tag{13}$$

In these functions, n_i and N represent the number of training data in the i^{th} class and the total number of training data, respectively.

7.2. Simplified Discriminant Function

The method of the geochemical spectrum of elements was proposed to determine and calculate the discriminant function. This method can separate different rocks in terms of geochemistry. It also separates similar formations in terms of having or not having potential [17]. For the first time, Solovov presented the method of the geochemical spectrum for comparing two similar geochemical fields with different economical natures using simple graphical charts [18]. The results of these two Russian researchers [17 and 18] show that calculating the discriminant function using mathematical methods is usually not comprehensive in representing geological models; therefore, they believe that the discriminant function should be simple. Accordingly, if we have two homogeneous or similar formations or fields (I, II), and using one of the simplest discriminant functions with two variables C_1 and C_2, we obtain the following linear function [17].

$$v = \frac{(C_1)_I}{(C_1)_{II}} \tag{14}$$

This linear function in geochemical fields is called the 'segregation index', which can be illustrated by a two-dimensional plot between these two mentioned variables. This function can belong to class II for any unknown sample with the following conditions [17].

$$v = \frac{(C_1)_I}{(C_1)_{II}} \prec 1 \tag{15}$$

and in case:

$$v = \frac{(C_1)_I}{(C_1)_{II}} \succ 1 \tag{16}$$

It belongs to class I. Thus, the separation of these two classes is possible by a simple linear discriminant function in a 2D chart. However, in a 1D chart, the separation of these two classes with two or more variables is not possible. The extension of this graphical method in two similar classes (each with several variables) is known as the 'geochemical spectrum method'. The segregation index v is a parameter which is separately calculated for each class, and if the ratio $\nu_1/\nu_2 > 1.0$ is satisfied, this determines the difference in the chemical combination between these two similar classes [17].

7.3. Graphical Representation of the Discriminant Function

In order to compare two similar classes and extract the discriminant function between two standard classes and the target class, the Solovov graphical method was employed. First, the chart of the standard geochemical spectrum of the different classes with several variables was sketched (the longitudinal axis) from ascending to descending values, and we then sketched the geochemical spectrum chart for similar variables versus the standard curve. If the charts coincide perfectly, these two classes are similar in terms of their potential or chemical compositions, even if the absolute values of these variables exhibit considerable differences.

7.4. Selecting Strong and Weak Index Formations

As mentioned before, in this method the strongest and weakest data for each class are used to obtain a discriminant parameter. According to our studies, it was noted that the TOC content has particular importance in shaly source rocks; therefore, the samples with a low TOC percentage d not operate as the main parameter in these sources. The maturity of the organic sample is also important and can be determined by the two parameters T_{max} and R_o. In order to find the good and the bad classes, these parameters were studied in shaly formations.

7.4.1. Optimal Selection of Structures Based on the Discriminant Analysis Model

Using discriminant analysis has some complexity and it is necessary to find an easier technique to take its advantage; therefore, a graphical calculation of discriminant analysis was proposed.

7.4.2. Development of the Discriminant Parameter

The discrimination parameter should separate two communities; therefore, finding a parameter that represents the best difference between good and bad communities is the goal of this section. Here, a simple graphical method of separation is used to achieve the best parameter. Since this method uses linear regression, it can be expressed as follows.

$$DA = \frac{x_1 * x_2 * ... * x_n}{y_1 * y_2 * ... * y_n} \tag{17}$$

where x and y are the geochemical parameters determined as the discriminant parameter. It is important to note that the number of parameters in the numerator and denominator must be equal - in other words, the sum of the numerator and denominator power must be equal. Thus, among the geometrical parameters, each parameter that satisfied these conditions can be selected to find the best separation between the data of these two formations. To draw a graphical distinction analysis, initially and for good samples (Garau), the geochemical values are sorted in descending order from small to large quantities. Hence, these parameters from are T_{max}, HI, OI, PP, TOC, S2, S1, Ro, MI and PI.

In Figure 17, the parameters are set out for both good and bad communities. Since the separation of the dots in this method is important, we use a semi-log plot.

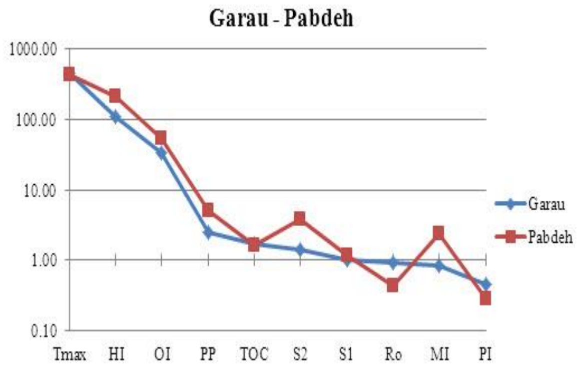

Fig. 17. Semi-log diagram of the Garau and Pabdeh parameters.

Figure 17 is used for determination of x and y in Eq. 17. The parameters of Figure 17 comprise the x value when they have less population in poor community (Pabdeh) than the strong community, and vice versa, to make up the y value. Here, the parameters T_{max}, TOC, Ro and PI constitute x1 to x4 and the parameters HI, OI, PP, S2 and S1 determine y1 to y6. Among the mentioned geochemical parameters, since S1 indicates the free hydrocarbons in the rock, and due to the migration of hydrocarbons from other formations, their values vary in different parts and as such it is removed from the list of parameters.

Thus, there are four parameters in the numerator and five parameters in the denominator of the fraction. Here, by using the trial and error method and testing different parameters, we attempt to obtain the best separation parameter.

Eq. 18 is an example of a discriminant factor.

$$DF_1 = \frac{T_{max} * TOC * PI * RO}{HI * PP * S2 * MI} \tag{18}$$

The value of this factor was calculated for both good and bad samples.

$$DF_1(Garau) = \frac{446.6 \times 1.7 \times 0.46 \times 0.94}{107.59 \times 2.53 \times 1.39 \times 0.84} = 1.0316713 \tag{19}$$

$$DF_1(Pabdeh) = \frac{428.17 \times 1.64 \times 0.28 \times 0.428}{211 \times 5.03 \times 3.84 \times 2.34} = 0.0088 \tag{20}$$

With this method, the ratio between the factors of both good and bad communities illustrates better separation. Thus, by changing the parameters and their power, the best factor showing the maximum value between the two communities is achieved. Here, the DF1 ratio between the Garau and Pabdeh factors is 117.235.

It is worth mentioning that the powers of these parameters should be positive. Eqs. 21- 28 show different factors, including PI, S2, MI and R_O, with different forms of exponent.

$$DF_2 = \frac{T_{max} * TOC * (PI^2) * RO}{HI * PP * S2 * (MI^2)} \tag{21}$$

DF_2 (Garau) = 0.5649628

DF_2 (Pabdeh) = 0.0010534

DF_2 = 536.326

$$DF_3 = \frac{T_{max} * TOC * (PI^2) * RO}{HI * PP * (S2^2) * MI} \tag{22}$$

DF_3 (Garau) = 0.3414164

DF_3 (Pabdeh) = 0.0006419

DF_3 = 531.874

$$DF_4 = \frac{T_{max} * TOC * PI * (RO^2)}{HI * PP * (S2^2) * MI} \quad (23)$$

DF_4 = 712.704

$$DF_5 = \frac{(T_{max}{}^2) * TOC * PI * RO}{HI * PP * S2 * (MI^2)} \quad (24)$$

DF_5 = 340.099

$$DF_6 = \frac{T_{max} * (TOC^2) * PI * RO}{HI * PP * (S2^2) * MI} \quad (25)$$

DF_6 = 335.594

$$DF_7 = \frac{T_{max} * TOC * (PI^2) * RO}{HI * (PP^2) * S2 * MI} \quad (26)$$

DF_7 =382.772

$$DF_8 = \frac{T_{max} * TOC * (PI^2) * (RO^2)}{HI * (PP^2) * S2 * (MI^2)} \quad (27)$$

DF_8 =2347.3438

$$DF_9 = \frac{T_{max} * TOC * (PI^2) * (RO^2)}{HI * PP * (S2^2) * (MI^2)} \quad (28)$$

DF_9 =3261.7125

The OI can be considered a good indicator. Therefore, the PP parameter in DF2-DF9 was replaced with the OI. The obtained results are shown in Table 5. All nine factors demonstrate acceptable accuracy for the division of the samples. To select the most efficient factor, they were applied to the data.

Table 5. Discriminant factors with PP and OI.

	PP	OI
DF_2	536.326	435.517
DF_3	531.874	431.902
DF_4	712.704	578.742
DF_5	340.099	276.174
DF_6	335.594	272.515
DF_7	382.772	252.402
DF_8	2347.343	1547.851
DF_9	3261.712	2648.634

7.4.3. Separating Good and Bad Communities through the Discriminant Parameter

As mentioned before, the goal of finding these factors is to separate the communities from one another other such that, when an unknown sample is analysed using that factor, the result is good enough to determine the community of that sample or which community it is closer to. According to what has been expressed, these factors are obtained based on the mean values of the geochemical parameters, and if knowledge of the real difference between these factors is needed, it should be applied to each sample and the results should be compared. The discriminant function assigns a number (a discriminant factor) for each sample of the case study based on geochemical parameters. The discriminant factor must have the ability to separate the values of the two communities in two different numerical ranges. Thus, if the values of the discriminant factor of the bad and the good communities are compared, they must show a distinction between the two communities.

For this purpose, the discriminant factors of all the samples of the Garau and Pabdeh formations were calculated and then the frequencies of the discriminant factor values in the two communities were compared with one another other. Figures 18 and 19 show this comparison. Figure 18a is drawn based on DF_1. It shows that approximately 90% of the values of the good community (Garau) are higher than 0.1, and that 75% of the values of the bad community (Pabdeh) are lower than 2. It shows the low quality of isolation. Around 50% of the values of these two communities also overlap with each other. Thus, it has a low efficiency factor. Some of the points for each_community are not in a same line as the samples of the whole community. These samples are 20-25% values of the Pabdeh samples that their discriminant factor is higher than 2. In Figure 18b, the overlapping rate of the Pabdeh and Garau formations is high (62%). This clearly indicates the low ability of DF_2 to isolate the two communities. Figure 18c shows DF_3, which can largely isolate the two communities. The overlapping rate of the two diagrams is nearly 30%. In fact, we can say that 89% of the values of factor three are higher than 0.1 for the Garau formation and 88% of the values of factor three are lower than 0.1. Hence, DF_3 could isolate the two communities. Therefore, the diagram of the values of factor three has been drawn in Figure 18d for two other communities, i.e., the Kazhdumi and Sargelu formations, to measure the efficiency of this factor. As expected, the two communities have been separated very well and the overlapping rate is less than 10%. DF_4 is shown in Figure 18e, in which the poor community values (Pabdeh) are mostly below 1 while the values of the Garau formation vary from 0.001 to 1000 and there is a large overlap between the two communities (approximately 48%). Figure 18f shows the values of DF_4 in which the PP has been replaced with the OI. In this diagram, a more complete isolation has occurred. This means that 88.8% of the values of the poor community (Pabdeh) are lower than 0.1 and 78% of the values of the strong community (Garau) are above 0.1.

The parameter of DF_4 (OI) has been drawn for the Kazhdumi and Sargelu formations in Figure 18g. The overlapping rate between the two communities is very low, at approximately 12%. DF_5 is shown in Figure 18h. Unlike the other samples, the Pabdeh values are very high and 65% are higher than 100. Because, T_{max} in this factor is extended to power two. This factor clearly does not work.

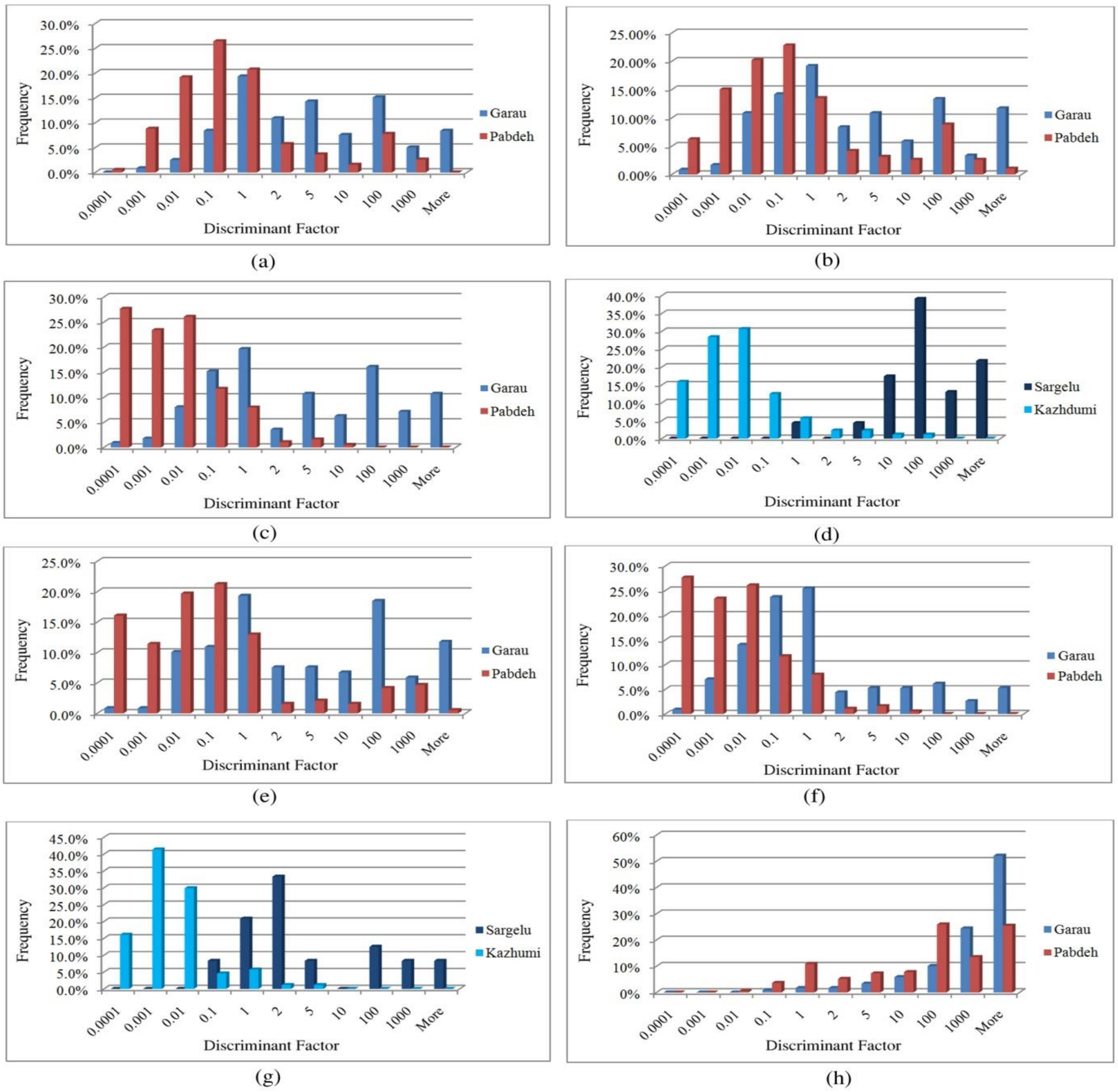

Fig. 18. Frequency of the different discriminant factors in the studied formation.

Factor 6 is shown in Figure 19a. The overlapping rate between the two diagrams is approximately 50%. Figure 19b shows a poor isolation. It occurred through DF_7, and the overlapping rate between the two diagrams is approximately 50%. DF_7 (OI) in Figure 19c clearly shows that 98% of the values of the Pabdeh samples are below 0.01 and that 94% of the values of the Garau formation is above 0.001. This factor a strong ability to differentiate the two communities, while the overlapping rate of the two communities is 33% (which is considerable). DF_7 is shown in Figure 19d by replacing OI with PP and with the values of this factor for the Kazhdumi and Sargelu formations. This diagram shows that the Sargelu and Kazhdumi formations exhibit two different behaviours but have considerable overlap (37%). Figure 19e shows that there is almost no separation between the two communities. Figure 19f shows DF_8 (OI), and in this diagram 96.9% of the values for Pabdeh are below 0.1, among which 71% are below 0.0001, which is a good indicator of a poor community (a good index to identify a poor community) though it is not a good factor to discriminate between the two communities. Factor 9 in Figure 20g does not show a clear separation between the two communities.

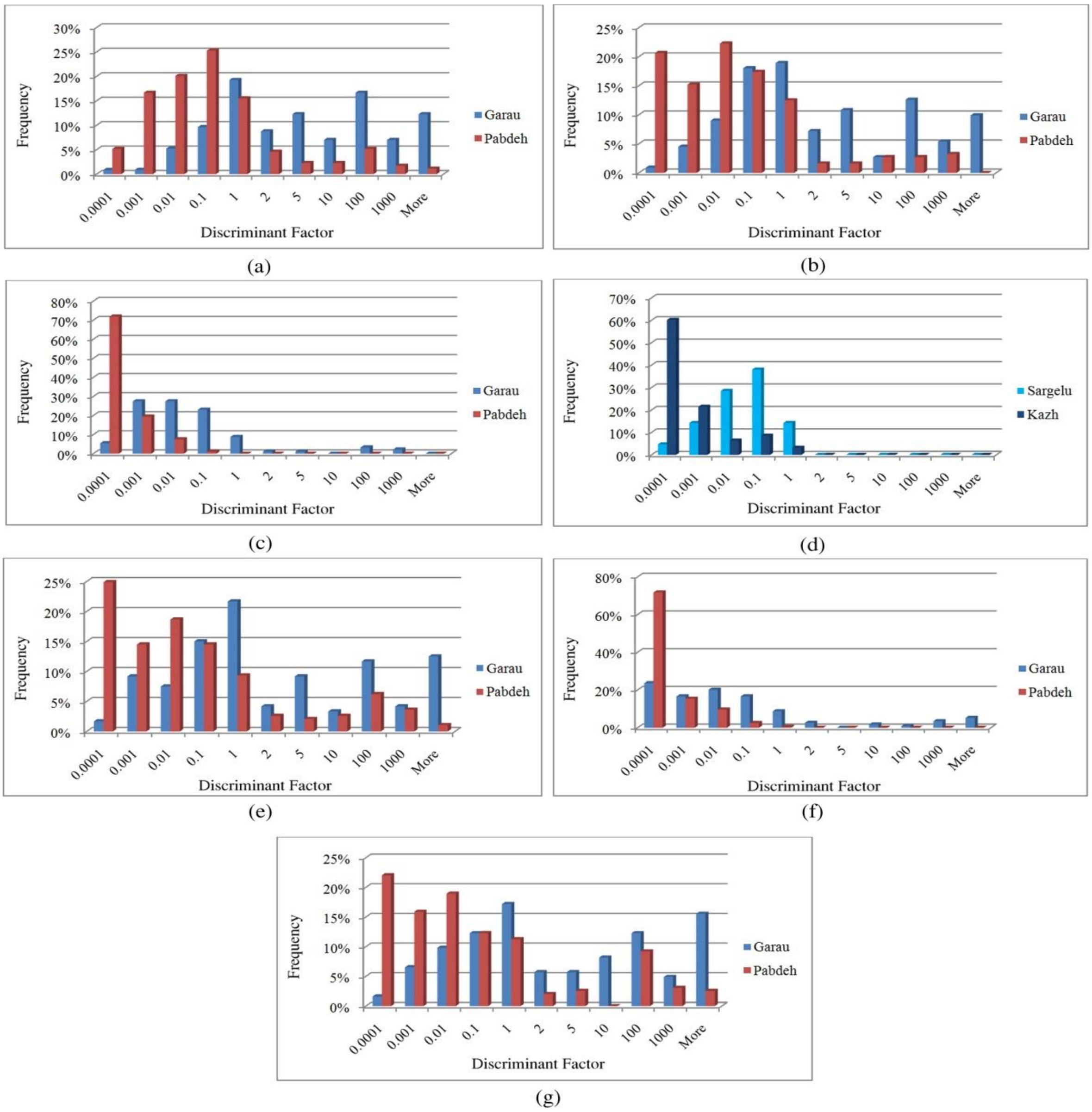

Fig. 19. Frequency of different discriminant factors in the studied formations.

8. Conclusions

The graphical representation of discriminant analysis was used to develop a statistical-mathematical model for the classification of probable source rocks in the Lorestan basin. Rock-Eval parameters, including T_{max}, TOC, PI, Ro, HI, PP, S2 and MI, were used to develop a discriminant function. All of the studied formations show that the mean value of the TOC is high in the Lorestan basin while their individual thermal maturity differs considerably. Based on R_O and T_{max} data, the Sargelu and Pabdeh formations represent the most mature and immature formations, respectively. The Garau formation was selected as good community based on the statistical analysis of the geochemical parameters. On the other hand, the Pabdeh formation is representative of a bad community. Various discriminant parameters were developed through the discriminant function, and among them the potential of 12 parameters for separating good and bad communities was investigated. Parameter DF_3 showed acceptable separation such that the overlap of the two communities was less than 30%. The value of this factor for 89% of the Garau formation is greater than 0.1 while for 88% of the Pabdeh formation it is less than 0.1. This fact confirms the acceptable performance of its discriminant role. Parameters DF_7 and DF_8 performed acceptably in designating the samples of the weak community whereas they were not suitable for separating any two communities. The discriminant parameters of this research were obtained based on available information of the geochemical characteristics of studied formations. Using a database of other formations and hydrocarbon fields would certainly help to improve the performance and capabilities of the discriminant parameters. If this were to be the case, the obtained discriminate parameters could be used to study other formations.

Acknowledgments

We would like to express our gratitude to Dr. Masoud Nemati from the Research Institute of the Petroleum Industry (RIPI) for his assistance with this study. Many thanks are also due to M. Aqa Baba Goli and Behnam Hami for their support and help. In addition, we extend our appreciation to the Iranian Central Oil Fields Company (ICOFC) for its support during this research.

References

[1] Motiei, H. (1993). Stratigraphy of Zagros, Hushmandzadeh A. (ed.) Treatise on the Geology of Iran, Geological Survey of Iran, Tehran, 536 p. (in Farsi).

[2] Ashkan, S.A.M. (2004). Fundamentals of geochemical studies of Hydrocarbon source rocks and oils with special look at the sedimentary basin of Zagros, Natioinal Iranian Oil Company, 355p.

[3] Bordenave, M.L. and Burwood, R. (1990). Source rock distribution and maturation in the belt, provenance of the Asmari and Sarvak reservoirs oil accumulations, Journal of Organic Geochemistry, 16, pp. 369-387.

[4] Sepahvand, S. (2002). Reconnaissance of Kazhdumi Formation Biomarkers as Asmari and Bangestan Pertroleum Reservoirs Probable Source Rock, Thesis of Master of Science in petroleum geochemistry, Ramhormoz University, Department of science, (In Farsi). 250p.

[5] Schultz, R.B. (2004). Geochemical relationships of Late Paleozoic carbon-rich shales of the Midcontinent, USA: a compendium of results advocating changeable geochemical conditions. Chemical Geology 206, pp. 347–372.

[6] Wang, G. and Carr, T.R. (2012). Methodology of organic-rich shale lithofacies identification and prediction: A case study from Marcellus Shale in the Appalachian basin. Computers & Geosciences, 49, pp. 151–163.

[7] Peh, Z. and Halamić, J. (2010). Discriminant function model as a tool for classification of stratigraphically undefined radiolarian cherts in ophiolite zones, Journal of Geochemical Exploration, 107, pp. 30–38.

[8] Caetano Bicalho, C., Batiot-Guilhe, C., Seidel, J.L., Van Exter, S., Jourde, H., (2012). Geochemical evidence of water source characterization and hydrodynamic responses in a karst aquifer, Journal of Hydrology, 450-451, pp. 206–218.

[9] Ujević Bošnjak, M., Capak, K., Jazbec, A., Casiot, C., Sipos, L., Poljak, V. and Dadić, Ž. (2012). Hydrochemical characterization of arsenic contaminated alluvial aquifers in Eastern Croatia using multivariate statistical

techniques and arsenic risk assessment, Science of the Total Environment, 420, pp. 100–110.

[10] Ghiasi-Freez, J., Soleymanpour, I., Kadkhodaie-Ilkhchi, A., Ziaii, M., Sedighi, M. and Hatampour, A. (2012). Automated Porosity Identification from Thin Section Images Using Image Analysis and Intelligent Discriminant Classifiers, Journal of Computers & Geosciences, 45, pp. 36-45.

[11] James, G.A., and Wynd, J.G. (1965). Stratigraphic Nomenclature of Iranian Oil Consortium Agreement Area. AAPG Bulletin, 49(12).

[12] Kavoosi, M.A., Daryabande, M., Jamali, A.M., Bagheri, R., Ebadian, H. and Sherkati, Sh. (2011). Primary tracking of unconventional hydrocarbons reserves of shale gas in Iran, The report of NIOC, TR1914, Unpublished. (In Farsi).

[13] Tissot, B.P. and Welte, D.H. (1984). Petroleum Formation and Occurrence, Second Revised and Enlarged Edition.

[14] McCarthy, K., Rojas, K., Neimann, M., Palmowski, D., Peters, K. and Stankiewicz, A. (2011). Basic Petroleum Geochemistry for Source Rock Evaluation, Schlimberger Oilfield review summer, No. 2.

[15] Peters, K.E. and Cassa, M.R. (1994). Applied Source Rock Geochemistry, Magoon, L.B., Dow, W.G. (Eds.), The Petroleum System – from Source to Trap. AAPG Memoir, 60, pp. 93–120.

[16] Skret, U. and Fabianska, M.J. (2009). Geochemical characteristics of organic matter in the Lower Palaeozoic rocks of the Peribaltic Syneclise (Poland), Geochemical Journal, 43, pp. 343-369.

[17] Beus, A.A. and Grigorian, S.V. (1977). Geochemical Exploration Methods for Mineral Deposits, Applied Publishing, Wilmette, IL, translated from Russian, 287p.

[18] Solovov, A.P. (1987). Geochemical Prospecting for Mineral Deposits. Mir, Moscow, 288 pp. V.V. Kuznetsov, Trans.; Engl. ed.

[19] Hastie, T., Tibshirani, R. and Friedman, J. (2001). The elements of statistical learning, Springer Series in Statistics, Springer.